Second-order two-scale computations for conductive–radiative heat transfer problem in periodic porous materials*

Yang Zhi-Qiang(杨志强)[a)†], Cui Jun-Zhi(崔俊芝)[b)], and Li Bo-Wen(李博文)[b)]

[a)] *Department of Applied Mathematics, Northwestern Polytechnical University, Xi'an* 710129, *China*
[b)] *LSEC, ICMSEC, Academy of Mathematics and Systems Sciences, Chinese Academy of Sciences, Beijing* 100190, *China*

(Received 16 May 2013; revised manuscript received 7 August 2013; published online 12 February 2014)

In this paper, a kind of second-order two-scale (SOTS) computation is developed for conductive–radiative heat transfer problem in periodic porous materials. First of all, by the asymptotic expansion of the temperature field, the cell problem, homogenization problem, and second-order correctors are obtained successively. Then, the corresponding finite element algorithms are proposed. Finally, some numerical results are presented and compared with theoretical results. The numerical results of the proposed algorithm conform with those of the FE algorithm well, demonstrating the accuracy of the present method and its potential applications in thermal engineering of porous materials.

Keywords: second-order two-scale (SOTS) computations, periodic porous materials, conductive–radiative heat transfer

PACS: 02.30.Jr, 44.40.+a, 02.60.–x, 02.60.Cb **DOI:** 10.1088/1674-1056/23/3/030203

1. Introduction

Porous materials have many elegant properties, such as low relative density and heat insulation, and have been widely used in a variety of industrial products. These kinds of materials have small pores that may be open, connected, or closed, and often subjected to thermal or chemical influence at internal and external boundaries. As the materials often have periodic configurations and characteristic coefficients oscillate rapidly in small cells, it is necessary to develop a new kind of effective numerical method to predict the physical and mechanical performance.

Radiation plays an important role in heat transfer at high temperature. Some authors have developed numerical and theoretical methods for predicting the thermal properties of the problem. Liu and Zhang[1] predicted the macroscopic properties of the heat conduction–radiation problem. Tiihonen[2] discussed radiation on non-convex surfaces, and proved the existence and uniqueness of the stationary conduction radiation problem. Bakhvalov[3] studied an averaging method on the heat transfer process inside periodic medium with radiation and gave the asymptotic expansion of the temperature. Convection occurs by flow, and can be neglected at low pressures or in closed-cell porous materials.[1,4] However, it manifests significantly in heat transfer as the pores are large or connected.[5] Recently, EI Ganaoui[6] dealt with a linear heat conduction problem with convection boundary condition using the first-order asymptotic expansion. However, its convergence was not shown there. Later, Terada *et al.*[7] considered the scale effect of a unit cell and derived formal expansions for the thermo–mechanical problem by the homogenization method. In addition, the scale effect induced by the pore size in heat transfer and mass diffusion of porous materials were pointed out in Refs. [8]–[10].

In the study of the asymptotic analysis of the heat transfer model, there are few results concerning the conduction convection and radiation heat transfer problem comprehensively. In Refs. [11] and [12], the authors considered a linear heat conduction equation with ε^{-1}-order radiation boundary conditions by two-scale asymptotic expansion, and justified the convergence. It should be noticed that this non-classical model cannot be used for the materials with low porosity, because it overestimates the radiation behavior on the interior surface of cavities. Later, Yang *et al.*[13] gave a second-order two-scale method to solve the coupled conduction and radiation equation with rapidly oscillatory coefficients, but did not consider the effect of convection.

It should be pointed out that the homogenization method only describes the asymptotic behavior of the problems as $\varepsilon \to 0$. However, in practical engineering computation, ε does not approach zero, and actually it is not very small. Substituting the first-order two-scale solution into the original equation, we can find that the residual is $O(1)$ even though H^1-norm of its error is $O(\varepsilon^{1/2})$. The local error $O(1)$ is not acceptable for engineers who want to capture the local behavior of the solution. Therefore, it is necessary to seek the higher-order asymptotic methods.

According to the homogenization methods,[14,15] Cui *et al.*[16–18] and He *et al.*[19,20] presented a higher-order multi-

*Project supported by the National Basic Research Program of China (Grant No. 2010CB832702) and the National Natural Science Foundation of China (Grant No. 90916027).

†Corresponding author. E-mail: yangzhiqiang@mail.nwpu.edu.cn

© 2014 Chinese Physical Society and IOP Publishing Ltd

scale analysis method to predict the physical and mechanical properties of composite materials and solved some practical problems. With the help of higher-order correctors, the microscopic fluctuations of physical and mechanical behaviors inside the material can be captured more accurately. As the sizes of man-made devices and structures have been reduced down to the nanoscale, the physical principles governing their operation are changed dramatically. Different kinds of multiscale methods are required. Luo and Cao[21] provided a framework for the coupled atomistic-continuum simulations for the heat transfer problem. Meanwhile, Shao *et al.*[22] and Yu and Wang[23] developed a multiscale method for the atomic scale simulation.

In this paper, we mainly discuss the conductive–radiative heat transfer behavior in a three-dimensional (3D) domain, periodically perforated by thin parallel pipes in which fluid is flowing. Heat convection occurs in the fluid which is assumed to be transparent for radiation, while the radiation acts on the surfaces of cavities and the pipes walls. The goal of this paper is to establish a new numerical method to offer a better approximation. We introduce the higher-order correction terms into the asymptotic expansion of the temperature field, and then derive a family of cell problems. A new SOTS method is utilized to predict heat transfer performances of periodic porous materials.

The remainder of this paper is organized as follows. In Section 2, the second-order asymptotic expansions for the heat transfer problem that accounts for the scale effect of unit cell are derived. In Section 3 the algorithm procedure and some numerical results for the heat transfer problem are shown. In the last section, some concluding remarks are presented.

Throughout this paper the Einstein summation convention on repeated indices is adopted.

2. Second-order two-scale formulation

In this section, the SOTS formulation is derived for calculating the thermal properties, including heat conduction parameters and temperature fields.

Let $Y = \{y : 0 \le y_j \le 1, j = 1,2,3\}$ and ω be an unbounded domain of R^3 which satisfies the following conditions:

(i) ω is a smooth unbounded domain of R^3 with a 1-periodic structure;

(ii) the cell of periodicity $Y^* = \omega \cap Y$ is a subdomain with a Lipschitz boundary, where Y^* is the reference periodicity cell, as shown in Fig. 1(b);

(iii) the set $Y \backslash \bar{\omega}$ and the intersection of $Y \backslash \bar{\omega}$ with the δ_0 neighborhood of ∂Y consist of a finite number of Lipschitz domains which are separated from each other and apart from the edges of the cube Y by a positive distance;

(iv) the cavities the pipes are convex.

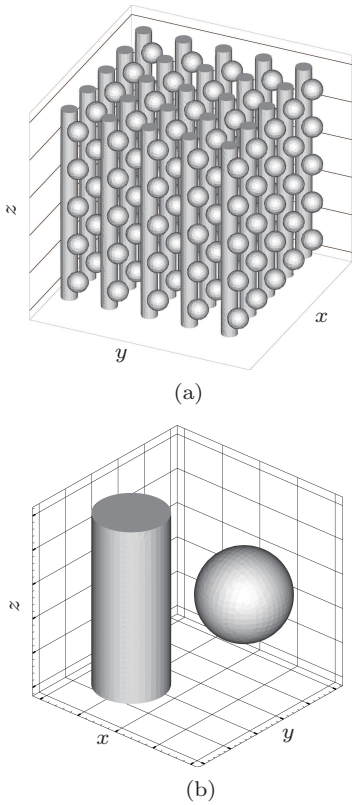


Fig. 1. Periodic distribution of porous materials. (a) Domain Ω^ε; (b) unit cell Y^*.

Then, the domain Ω^ε shown in Fig. 1(a) has the form: $\Omega^\varepsilon = \Omega \cap \varepsilon\omega$, and $\partial\Omega^\varepsilon = \partial\Omega \cup \Gamma_\varepsilon^1 \cup \Gamma_\varepsilon^2$, where Ω is a bounded Lipschitz convex domain of R^3 without cavities and pipes, and Γ_ε^2 denotes the surfaces of cavities. The domain Ω^ε has pipes with the axis in the third direction, of which the diameter is of the same order as the period. Let Γ_ε^1 denote the wall of the pipes γ_ε the bottom boundary of all pipes Γ_ε^1, Γ_ε the interior boundary that is composed of the wall of each pipe $\Gamma_{\varepsilon,i}^1$ and the surface of cavity $\Gamma_{\varepsilon,j}^2$, then we will have the following relationship:

$$\gamma_\varepsilon = \bigcup_{i=1}^{m(\varepsilon)} \gamma_{\varepsilon,i}, \quad \Gamma_\varepsilon^1 = \gamma_\varepsilon \times (0, L_3),$$

$$\Gamma_\varepsilon = \bigcup_k \Gamma_{\varepsilon,k} = \Gamma_\varepsilon^1 \cup \Gamma_\varepsilon^2 = \sum_{i=1}^{m(\varepsilon)} \Gamma_{\varepsilon,i}^1 \bigcup \sum_{j=1}^{n(\varepsilon)} \Gamma_{\varepsilon,j}^2.$$

The fluid is assumed to be almost transparent. Moreover, we suppose that the radiative surfaces are diffuse and grey, that is, the emissivity e of the surfaces does not depend on the wavelength of the radiation, and that surface emits, absorbs, and reflects radiation in the same manner for all directions.

The heat conduction equation with surface radiation was firstly studied by Bakhvalov,[3] and later by Liu and Zhang[1] Amosov,[24] and Yang *et al.*,[13] in which the radiation boundary condition in a closed cavity was essentially expressed as

$$-v_i k_{ij}^\varepsilon(x) \frac{\partial T_\varepsilon(x)}{\partial x_j} = e\sigma T_\varepsilon^4(x) - e \int_{\Gamma_{\varepsilon,i}} R_\varepsilon(z) F(x,z) \mathrm{d}z \text{ on } \Gamma_\varepsilon,$$

where σ is the Stefan–Boltzmann constant, v_i the unit outward normal on Γ_ε, and $R_\varepsilon(x)$ the intensity of emitted radiation defined by

$$R_\varepsilon(x) = e\sigma T_\varepsilon^4(x) + (1-e)\int_{\Gamma_{\varepsilon,i}} R_\varepsilon(z)F(x,z)\,\mathrm{d}z, \quad \forall x \in \Gamma_{\varepsilon,i}.$$

The classical radiation boundary condition is considered in this paper. Allaire and EI Ganaoui[11] considered the radiation condition with ε^{-1} scaling factor on Γ_ε. It must be noted that it is a mathematical hypothesis and the scaling ε^{-1} may not authentically reflect the physical behavior of the material when the porosity is low.

In addition, convection and diffusion take place in the pipes due to the fluid. It is further modeled by a fixed fluid temperature $T_\mathrm{f} \in H^1(\Omega^\varepsilon)$ and a heat exchange coefficient $h_\varepsilon(x)$. Then, in the absence of radiative transfer, the heat flux on the boundary is

$$-v_i k_{ij}^\varepsilon(x)\frac{\partial T_\varepsilon(x)}{\partial x_j} = \varepsilon h_\varepsilon(x)(T_\varepsilon(x) - T_\mathrm{f}) \ \text{ on } \ \Gamma_\varepsilon.$$

The scale effect on the homogenization for the heat transfer problem in porous materials is considered, which has been explained in more detail in Ref. [7].

Under the above assumptions, we consider the coupled equation for a given structure as follows:

$$\begin{cases} -\dfrac{\partial}{\partial x_i}\left(k_{ij}^\varepsilon(x)\dfrac{\partial T_\varepsilon(x)}{\partial x_j}\right) = f(x), & x \in \Omega^\varepsilon. \\ T_\varepsilon(x) = 0, & x \in \Gamma_1. \\ v_i k_{ij}^\varepsilon(x)\dfrac{\partial T_\varepsilon(x)}{\partial x_j} = 0, & x \in \Gamma_2. \\ -v_i k_{ij}^\varepsilon(x)\dfrac{\partial T_\varepsilon(x)}{\partial x_j} = G_\varepsilon(\sigma T_\varepsilon^4(x)) \\ \quad +\varepsilon h_\varepsilon(x)(T_\varepsilon(x) - T_\mathrm{f}), & x \in \Gamma_\varepsilon, \end{cases} \tag{1}$$

where $k_{ij}^\varepsilon(x)$ are the coefficients of thermal conductivity; $f(x)$ is the internal heat source; Γ_1 and Γ_2 denote boundary portions where temperature and heat flux are prescribed to ensure $\Gamma_1 \cup \Gamma_2 = \partial\Omega$ and $\Gamma_1 \cap \Gamma_2 = \emptyset$; and G_ε is the operator defined as[2,11]

$$G_\varepsilon(\sigma T_\varepsilon^4(x)) = e\sigma T_\varepsilon^4(x) - e\int_{\Gamma_{\varepsilon,i}} R_\varepsilon(z)F(x,z)\,\mathrm{d}z, \tag{2}$$

where $F(x,z)$ is the view factor between two different points x and z on $\Gamma_{\varepsilon,i}$, and is defined in the 3D form for a convex cavity as follows:

$$F(x,z) = F^{3\mathrm{D}}(x,z) = \frac{n_z(x-z)n_x(z-x)}{\pi|z-x|^4},$$

where n_z denotes the unit normal at the point z.

In the two-dimensional (2D) form, the view factor is

$$F(x,z) = F^{2\mathrm{D}}(x',z') = \frac{n'_z(x'-z')n'_x(z'-x')}{2|z'-x'|^3},$$

where x is the macroscopic coordinate of the structure and $x = (x', x_3)$.

Suppose that the following conditions are satisfied:

(v) $k_{ij}(x/\varepsilon) = k_{ji}(x/\varepsilon)$;

(vi) $k_{ij}(x/\varepsilon)$ are bounded, $\forall \eta \in \mathrm{R}^n$, and there exist two positive constants (c_1, c_2) such that

$$c_1|\eta|^2 \le k_{ij}(x/\varepsilon)\eta_i\eta_j \le c_2|\eta|^2;$$

(vii) $k_{ij}(y) = k_{ij}^\varepsilon(x)$ is 1-periodic functions in y, and $y = x/\varepsilon$;

(viii) $f \in L^2(\Omega^\varepsilon)$, $h_\varepsilon(x) \in L^2(\Omega^\varepsilon)$, $h_\varepsilon(x) \ge 0$.

Remark 1 Based on assumptions (vi)–(viii), the existence and uniqueness of the weak solution $T_\varepsilon(x)$ for the boundary value problem (1) can be established.[2,13]

To simplify the expansion, we assume that the emissivity is $e = 1$. However, our analysis can be extended straightforwardly to the case $0 < e < 1$.

We introduce a second-order two-scale asymptotic expansion for $T_\varepsilon(x)$ as follows:

$$\begin{aligned} T_\varepsilon(x) \ = \ & T_0(x) + \varepsilon N_{\alpha_1}(y)\frac{\partial T_0(x)}{\partial x_{\alpha_1}} + \varepsilon^2\Bigg(N_{\alpha_1\alpha_2}(y)\frac{\partial^2 T_0(x)}{\partial x_{\alpha_1}\partial x_{\alpha_2}} \\ & + C_{\alpha_1}(y)T_0^3\frac{\partial T_0(x)}{\partial x_{\alpha_1}} + C^1_{\alpha_1}(y)T_0^3(x)\frac{\partial T_0(x)}{\partial x_{\alpha_1}} \\ & + D(y)(T_0(x) - T_\mathrm{f})\Bigg) + \varepsilon^3 P_1(\varepsilon, x, y), \ x \in \varepsilon Y^* \subset \Omega^\varepsilon, \end{aligned} \tag{3}$$

where $T_0(x)$ is the homogenized solution that reveals the macro-characteristic of the problem; $N_{\alpha_1}(y)$, $N_{\alpha_1\alpha_2}(y)$, $C_{\alpha_1}(y)$, $C^1_{\alpha_1}(y)$, and $D(y)$ are the local solutions.

Next, we substitute the approximate solution (3) into Eq. (1). Aided by Lemma 2.1 in Ref. [12] and the formula

$$\frac{\partial}{\partial x} \to \frac{\partial}{\partial x} + \frac{1}{\varepsilon}\frac{\partial}{\partial y},$$

and equating the coefficients of the same powers for ε, from the ε^{-1} term we can obtain that $N_{\alpha_1}(y)$ is the solution of the following elliptic partial differential equation:

$$\begin{cases} \dfrac{\partial}{\partial y_i}\left(k_{ij}(y)\dfrac{\partial N_{\alpha_1}(y)}{\partial y_j}\right) = -\dfrac{\partial k_{i\alpha_1}(y)}{\partial y_i}, \ \text{in} \ Y^* \\ -v_i\left(k_{ij}(y)\dfrac{\partial N_{\alpha_1}(y)}{\partial y_j} + k_{i\alpha_1}(y)\right) = 0, \ y \in \Gamma \\ N_{\alpha_1}(y), \qquad\qquad Y: \ \text{periodic} \end{cases} \tag{4}$$

where $\Gamma = \Gamma^2 \cup \Gamma^1$ is the surface of the cavities and the walls of pipes contained in Y, and Y^* is the solid part of Y.

Define

$$\begin{aligned} \hat{k}_{ij} &= \frac{1}{|Y|}\int_{Y^*}\left(k_{i\mathrm{p}}(y)\frac{\partial N_j(y)}{\partial y_\mathrm{p}} + k_{ij}(y)\right)\mathrm{d}y, \\ \hat{h} &= \int_{\Gamma^1} h(y)\,\mathrm{d}\Gamma. \end{aligned} \tag{5}$$

Then, we can obtain the homogenized equation associated with Eq. (1) as follows:

$$\begin{cases} -\dfrac{\partial}{\partial x_i}\left(\hat{k}_{ij}\dfrac{\partial T_0}{\partial x_j}\right)+\dfrac{\hat{h}}{|Y|}(T_0-T_{\rm f})=\dfrac{|Y^*|}{|Y|}f, & \text{in } \Omega,\\ T_0=0, & \text{on } \Gamma_1,\\ v_i\hat{k}_{ij}\dfrac{\partial T_0}{\partial x_j}=0, & \text{on } \Gamma_2. \end{cases} \tag{6}$$

From assumption (vi) and Ref. [15], it follows that $\hat{k}_{ij}$ is symmetrical and positively definite. Then, the existence and uniqueness of the homogenization problem (6) can be obtained (see Ref. [6]).

From the ε^0 term, we can obtain auxiliary functions $N_{\alpha_1\alpha_2}(y)$, $C_{\alpha_1}(y)$, $C^1_{\alpha_1}(y)$, and $D(y)$. $N_{\alpha_1\alpha_2}(y)$ is the solution of the following problem:

$$\begin{cases} \dfrac{\partial}{\partial y_i}\left(k_{ij}(y)\dfrac{\partial N_{\alpha_1\alpha_2}(y)}{\partial y_j}\right)=\tilde{k}_{\alpha_1\alpha_2}\\ \quad -k_{\alpha_1\alpha_2}(y)-k_{\alpha_2 j}(y)\dfrac{\partial N_{\alpha_1}(y)}{\partial y_j}\\ \quad -\dfrac{\partial}{\partial y_i}\left(k_{i\alpha_2}(y)N_{\alpha_1}(y)\right), & \text{in } Y^*,\\ -v_i\Big(k_{ij}(y)\dfrac{\partial N_{\alpha_1\alpha_2}(y)}{\partial y_j}\\ \quad +k_{i\alpha_2}(y)N_{\alpha_1}(y)\Big)=0, & \text{on } \Gamma,\\ N_{\alpha_1\alpha_2}(y), & Y:\ \text{periodic}, \end{cases} \tag{7}$$

$C_{\alpha_1}(y)$ is the solution of the following problem:

$$\begin{cases} \dfrac{\partial}{\partial y_i}\left(k_{ij}(y)\dfrac{\partial C_{\alpha_1}(y)}{\partial y_j}\right)=0, & \text{in } Y^*,\\ -v_i\left(k_{ij}(y)\dfrac{\partial C_{\alpha_1}(y)}{\partial y_j}\right)=4\sigma\Big(N_{\alpha_1}(y)\\ \quad -\displaystyle\int_{\Gamma^2}N_{\alpha_1}(s)F^{\rm 3D}(y,s)\,{\rm d}s\Big), & y\in\Gamma^2\\ C_{\alpha_1}(y), & Y:\text{periodic}, \end{cases} \tag{8}$$

$C^1_{\alpha_1}(y)$ is the solution of the following problem:

$$\begin{cases} \dfrac{\partial}{\partial y_i}\left(k_{ij}(y)\dfrac{\partial C^1_{\alpha_1}(y)}{\partial y_j}\right)=0, & \text{in } Y^*,\\ -v_i\left(k_{ij}(y)\dfrac{\partial C^1_{\alpha_1}(y)}{\partial y_j}\right)=4\sigma\Big(N_{\alpha_1}(y)\\ \quad -\displaystyle\int_{\gamma}N_{\alpha_1}(s)F^{\rm 2D}(y',s')\,{\rm d}s'\Big), & y\in\Gamma^1,\\ C^1_{\alpha_1}(y), & Y:\text{periodic}, \end{cases} \tag{9}$$

$D(y)$ is the solution of the following problem:

$$\begin{cases} \dfrac{\partial}{\partial y_i}\left(k_{ij}(y)\dfrac{\partial D(y)}{\partial y_j}\right)=-\dfrac{\hat{h}}{|Y^*|}, & \text{in } Y^*,\\ -v_i\left(k_{ij}(y)\dfrac{\partial D(y)}{\partial y_j}\right)=h(y), & \text{on } \Gamma^1,\\ D(y), & Y:\text{periodic}, \end{cases} \tag{10}$$

where $\tilde{k}_{\alpha_1\alpha_2}=|Y|\hat{k}_{\alpha_1\alpha_2}/|Y^*|$.

Remark 2 Following the idea in Ref. [13], under assumptions (i)–(viii), the cell problems (4), and (7)–(10) admit a unique solution, up to a constant, in $H^1(Y^*)/R$.

Now we can define the two-scale approximate solution of problem (1) as follows:

$$\begin{aligned} T_1^\varepsilon(x) &= T_0(x)+\varepsilon N_{\alpha_1}(y)\frac{\partial T_0}{\partial x_{\alpha_1}},\\ T_2^\varepsilon(x) &= T_0(x)+\varepsilon N_{\alpha_1}(y)\frac{\partial T_0}{\partial x_{\alpha_1}}+\varepsilon^2\Big(N_{\alpha_1\alpha_2}(y)\frac{\partial^2 T_0}{\partial x_{\alpha_1}x_{\alpha_2}}\\ &\quad +C_{\alpha_1}(y)T_0^3\frac{\partial T_0}{\partial x_{\alpha_1}}+C^1_{\alpha_1}(y)T_0^3\frac{\partial T_0}{\partial x_{\alpha_1}}\\ &\quad +D(y)(T_0-T_{\rm f})\Big), \end{aligned} \tag{11}$$

where $T_1^\varepsilon(x)$ and $T_2^\varepsilon(x)$ are called the first-order and second-order two-scale approximate solution, respectively.

In summation, we can obtain the following theorem.

Theorem 1 The temperature field for the heat transfer problem (1) for porous material with periodic distribution has an SOTS asymptotic expansion as follows:

$$\begin{aligned} T_\varepsilon(x) &= T_0(x)+\varepsilon N_{\alpha_1}(y)\frac{\partial T_0}{\partial x_{\alpha_1}}+\varepsilon^2\Big(N_{\alpha_1\alpha_2}(y)\frac{\partial^2 T_0}{\partial x_{\alpha_1}\partial x_{\alpha_2}}\\ &\quad +C_{\alpha_1}(y)T_0^3\frac{\partial T_0}{\partial x_{\alpha_1}}+C^1_{\alpha_1}(y)T_0^3\frac{\partial T_0}{\partial x_{\alpha_1}}\\ &\quad +D(y)(T_0-T_{\rm f})\Big)+\varepsilon^3P_1(\varepsilon,x,y), \end{aligned} \tag{12}$$

where $T_0(x)$ is the solution of the homogenized equation (6); $N_{\alpha_1}(y)$, $N_{\alpha_1\alpha_2}(y)$, $C_{\alpha_1}(y)$, $C^1_{\alpha_1}(y)$, and $D(y)$ are the local solutions satisfying Eqs. (4), and (7)–(10), respectively.

Theorem 2 Suppose that $\Omega\subset {\rm R}^n$ $(n=1,2,3)$, is a bounded Lipschitz domain and $\partial\Omega\in {\rm C}^4$. Let $T_\varepsilon(x)$ be the solution of Eq. (1), $T_0(x)$ be the solution of homogenized equation (6), and $T_2^\varepsilon(x)$ be the approximate solution of Eq. (11). Under the assumptions (i)–(viii), if $f\in H^2(\Omega)$, for sufficiently smooth homogenized solutions $T_0(x)$, we obtain the following error estimate:

$$\|T_\varepsilon(x)-T_2^\varepsilon(x)\|_{H^1(\Omega^\varepsilon)}\le C\varepsilon^{1/2},$$

where C is a positive constant independent of ε.

Remark 3 In a way similar to that of proving Theorem 3.1 in Ref. [13], we can easily obtain the error estimate with $\varepsilon^{1/2}$ order under the regularity assumption of the homogenized solution. The main difficulty in obtaining the error estimate for the second-order two-scale approximate solution is how to treat the boundary conditions. We refer the readers to Ref. [13] for details.

3. FE algorithms and numerical examples

In this section, we describe the algorithm procedure to study the asymptotic behavior of the heat transfer problem (1) and present some numerical examples.

3.1. FE algorithms for the SOTS method

(1) Form and verify the geometry of the structure. Then, partition Y^* into FE mesh.

(2) Compute $N_{\alpha_1}(y)$ according to the problem (4) by the FE method. Furthermore, the homogenization coefficients $\hat{k}_{ij}$ and $\hat{h}$ are computed by using the formula (5).

(3) Given the computed $\hat{k}_{ij}$ and $\hat{h}$, the homogenization solution $T_0(x)$ is obtained by solving problem (6) in Ω.

(4) Applying the same meshes as those in (2), we evaluate $N_{\alpha_1\alpha_2}(y)$, $C_{\alpha_1}(y)$, $C^1_{\alpha_1}(y)$, and $D(y)$ by solving the cell problems (7)–(10).

(5) From Eq. (11), the temperature is evaluated.

3.2. Numerical examples

3.2.1. Example 1

Consider the mixed boundary value problem (1), where $\Omega^\varepsilon = [0, 0.25]^3$ is composed of entire cells shown in Fig. 1(a), and the reference cell $Y^* = [0, 1]^3$ is shown in Fig. 1(b). The boundary temperatures in the z direction are set to be T_1 and T_2. The values of emissivity of the cavity surfaces and pipe walls are equal to 1.0. $\sigma = 5.669996 \times 10^{-8}$ W/m^2·K^4, and the radii of the pipe and cavity in Y^* are 0.2 and 0.25, respectively. In addition, the radii of the pipe and cavity in Y^* are, respectively, 0.1 and 0.25 for Case 4 in the following.

Since it is difficult to find the analytical solution of Eq. (1), we have to take $T_\varepsilon(x)$ as their FE solution T_e in the very fine mesh, and implement the tetrahedron partition for Ω^ε. The number of elements and nodes are listed in Tables 1 and 2.

Table 1. Comparison of computational cost among different methods.

Elements	Original equation	Unit cell	Homogenized equation
	645800	5173	93750
Nodes	131726	1321	17576

Table 2. Comparison of computational cost among different methods for Case 4.

Elements	Original equation	Unit cell	Homogenized equation
	738945	5703	93750
Nodes	142241	1357	17576

The following four cases are investigated:

Case 1: $k_{ij0} = 1.9\delta_{ij}$, $h = 0.567$, $T_1 = 100$, $T_2 = 500$, $f = 0$;

Case 2: $k_{ij0} = 1.9\delta_{ij}$, $h = 0.567$, $T_1 = 100$, $T_2 = 1000$, $f = 0$;

Case 3: $k_{ij0} = 1.9\delta_{ij}$, $h = 0.0567$, $T_1 = 100$, $T_2 = 1000$, $f = 0$;

Case 4: $k_{ij0} = 100\delta_{ij}$, $h = 0.0567$, $T_1 = 100$, $T_2 = 1000$, $f = 1 \times 10^7$.

In order to show the thermal properties of porous materials, the effective thermal conductivity coefficients are obtained and the typical values for Cases 1 and 4 are

$$\begin{pmatrix} 1.6844 & 0.0137 & 0.0009 \\ 0.0137 & 1.6844 & 0.0004 \\ 0.0009 & 0.0004 & 1.8438 \end{pmatrix},$$

$$\begin{pmatrix} 95.9852 & 0.6077 & 0.0295 \\ 0.6077 & 96.1372 & 0.0406 \\ 0.0295 & 0.0406 & 97.3929 \end{pmatrix}.$$

It should be noted that $T_0(x)$ denotes the numerical solution for the modified homogenized equations (6) in a coarse mesh. $\hat{T}_1^\varepsilon(x)$ and $\hat{T}_2^\varepsilon(x)$ are the first-order and the second-order numerical solutions based on Eq. (3), respectively. Set the zeroth error $e_0 = T_\mathrm{e} - T_0(x)$, the first error $e_1 = T_\mathrm{e} - \hat{T}_1^\varepsilon(x)$, and the second error $e_2 = T_\mathrm{e} - \hat{T}_2^\varepsilon(x)$. For convenience, we introduce the following notation:

$$|v|_{H^1(\Omega^\varepsilon)} = \left(\int_{\Omega^\varepsilon} (|\nabla v|^2) \mathrm{d}x \right)^{1/2}.$$

The relative numerical errors of the homogenization, first-order, and second-order two-scale methods in the H^1 are listed in Table 3.

Table 3. Comparison of computing results of semi-norm H^1.

	$\lvert e_0\rvert_{H^1}/\lvert T_\mathrm{e}\rvert_{H^1}$	$\lvert e_1\rvert_{H^1}/\lvert T_\mathrm{e}\rvert_{H^1}$	$\lvert e_2\rvert_{H^1}/\lvert T_\mathrm{e}\rvert_{H^1}$
Case 1	0.16551096	0.04339014	0.04144399
Case 2	0.12593088	0.11078027	0.07717135
Case 3	0.12391140	0.10745522	0.07236294
Case 4	0.1662830	0.1042401	0.0702239

Figures 2(a)–2(f) illustrate the numerical results of $\hat{T}_1^\varepsilon(x)$, $\hat{T}_2^\varepsilon(x)$, and T_e at the intersection $x = 0.125$, and for $\partial\hat{T}_1^\varepsilon(x)/\partial y$, $\partial\hat{T}_2^\varepsilon(x)/\partial y$, and $\partial T_\mathrm{e}/\partial y$ at the intersection $y = 0.15$ in Case 2.

To check whether the second-order corrector is directly related to the amplitude of the source term (obvious in view of the cell problem (7) for $N_{\alpha_1\alpha_2}(y)$), we consider it in the numerical simulations.

Figures 3(a)–3(d) illustrate the numerical results for $T_0(x)$, $\hat{T}_1^\varepsilon(x)$, $\hat{T}_2^\varepsilon(x)$, and T_e at the intersection $z = 0.15$ in Case 4.

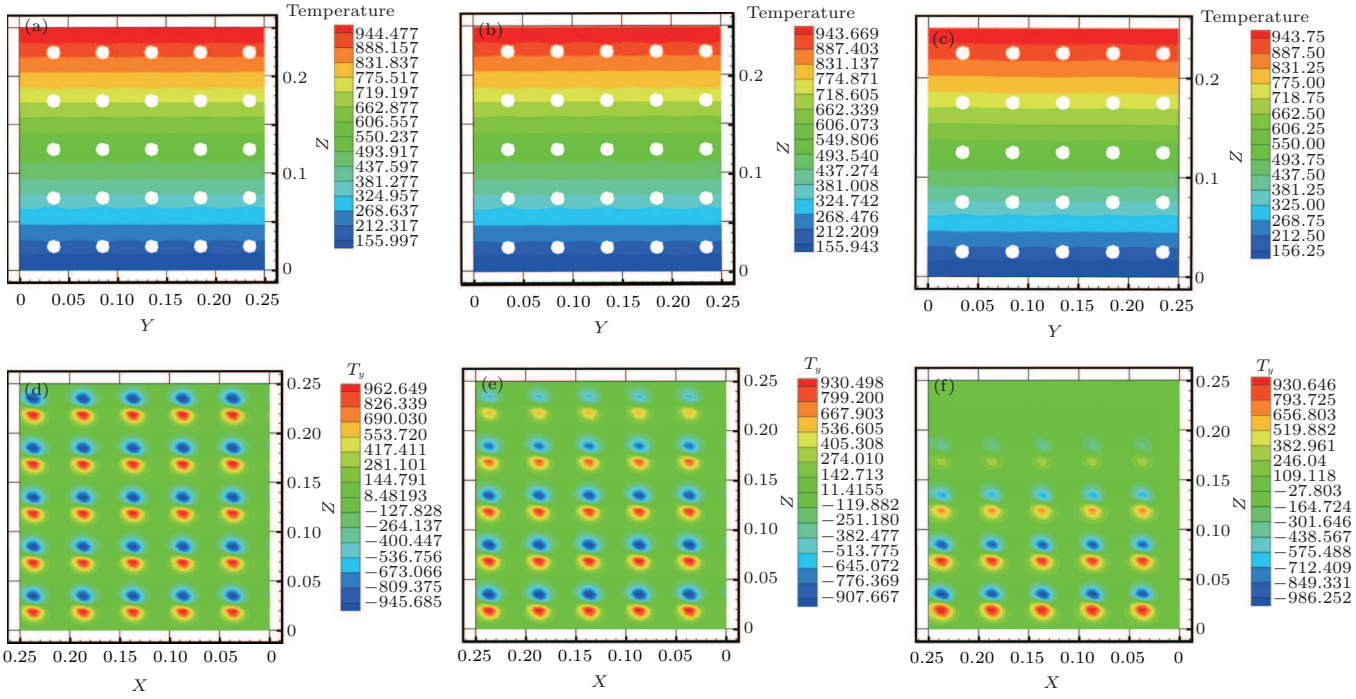


Fig. 2. (color online) (a) Case 2, $\hat{T}_1^{\varepsilon}(x)$; (b) Case 2, $\hat{T}_2^{\varepsilon}(x)$; (c) Case 2, $T_{\rm e}$; (d) Case 2, $\partial\hat{T}_1^{\varepsilon}(x)/\partial y$; (e) Case 2, $\partial\hat{T}_2^{\varepsilon}(x)/\partial y$; (f) Case 2, $\partial T_{\rm e}/\partial y$.

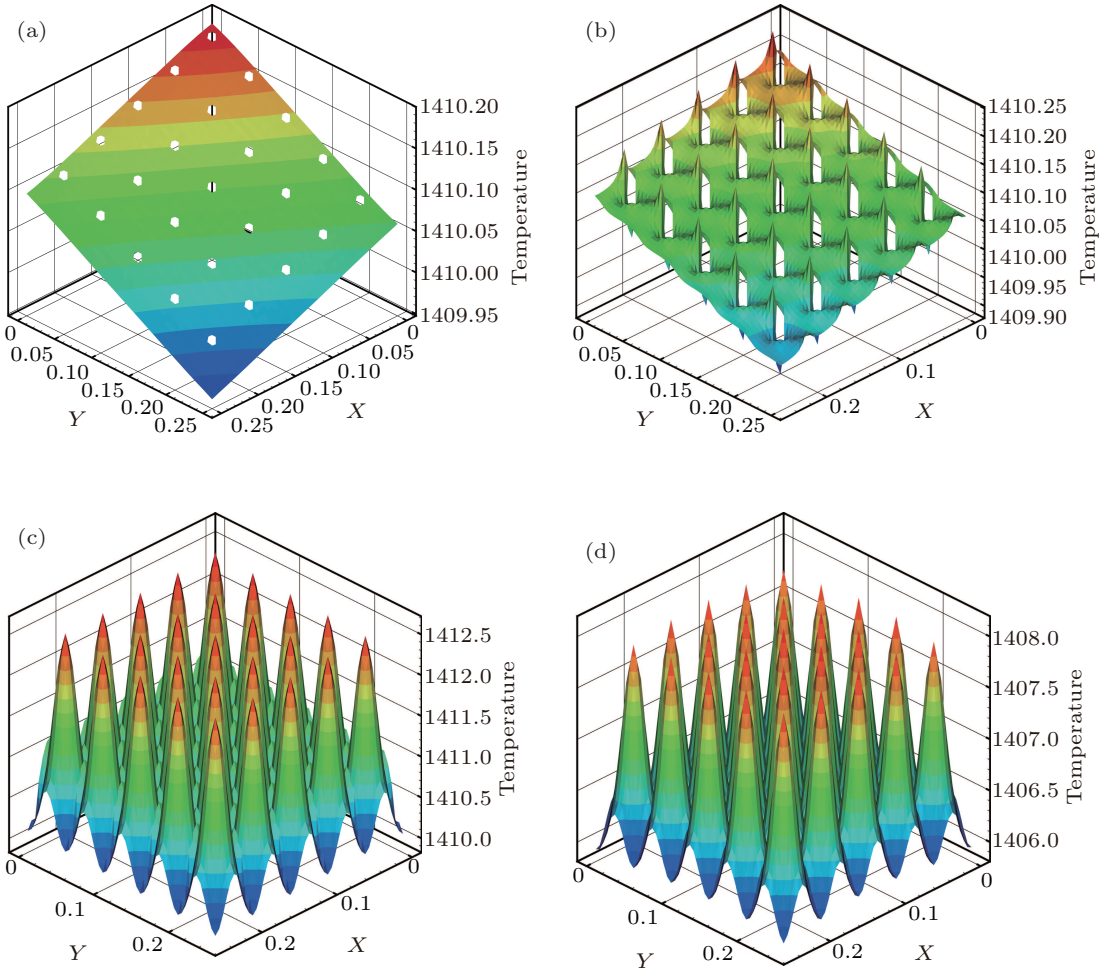


Fig. 3. (color online) (a) Case 4, $T_0(x)$; (b) Case 4, $\hat{T}_1^{\varepsilon}(x)$; (c) Case 4, $\hat{T}_2^{\varepsilon}(x)$; (d) Case 4, $T_{\rm e}$.

3.2.2. Example 2

In practical engineering, porous materials are generally comprised of a large number of pores. A porous system depicted in Fig. 4 is used to demonstrate the effectiveness of the SOTS computational method, which is composed of 8000 pores each with a diameter of $d = 6.25$ mm and 400 pipes each with a diameter of $d = 2.5$ mm, respectively. The thermal conductivity of the matrix is $k = 100$ W·K^{-1}·m^{-1} and the heat exchange coefficient is $h = 0.567$ W·K^{-1}·m^{-2} in pipes. The boundary temperatures in the z direction are set to be $T_1 = 100$ K and $T_2 = 800$ K. The internal heat source $f(x) = 10000$ M·W·m^{-3}. Figures 5(a)–5(d) illustrate the numerical results for $T_0(x)$, $\hat{T}_1^\varepsilon(x)$, $\hat{T}_2^\varepsilon(x)$, and T_e at the intersection $z = 0.1375$.

Both the SOTS method and the direct numerical simulations are performed on the same computer (with a memory size of 96 GB and 24 2.33-GHz processors). With the aid of the SOTS method, it is very time-saving to solve the simulation (3 s for solving the cell problem; about 35 s for the homogenized problem). Furthermore, the direct numerical simulation takes about 160 h to simulate the conductive–radiative heat transfer in this example because it requires fine meshes.

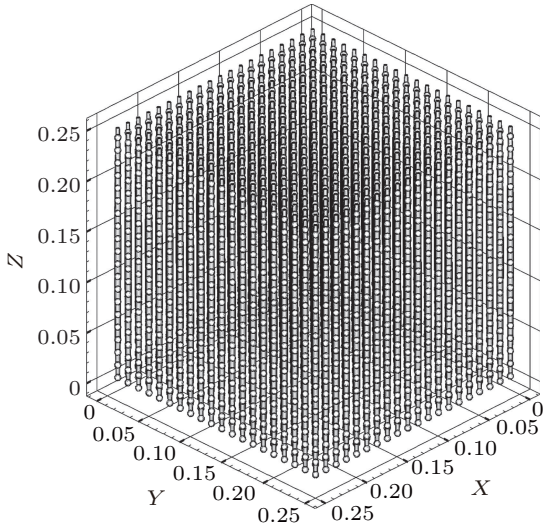


Fig. 4. Porous materials with a large number of pores. $\Omega^\varepsilon = [0, 0.25]^3$.

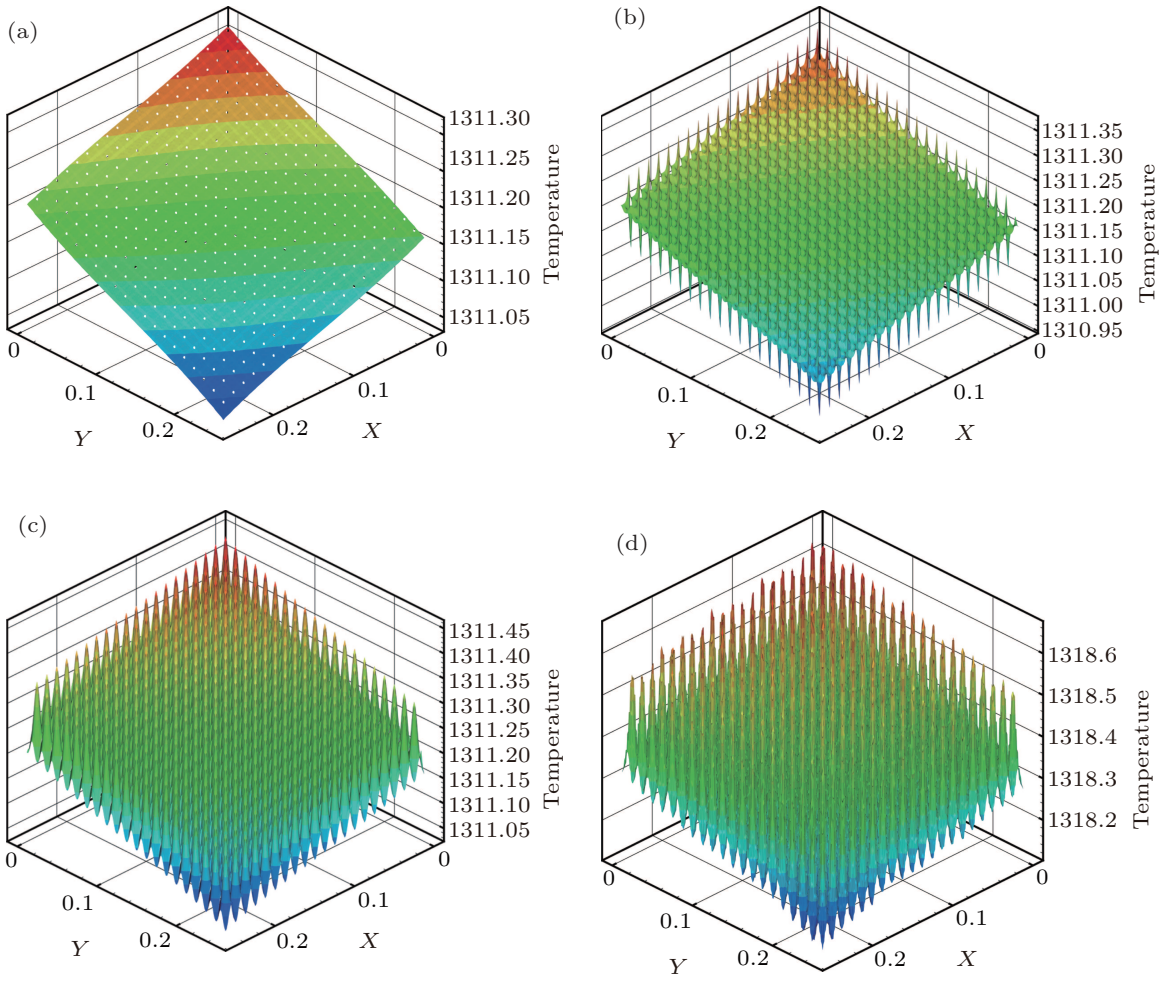


Fig. 5. (color online) (a) $T_0(x)$; (b) $\hat{T}_1^\varepsilon(x)$; (c) $\hat{T}_2^\varepsilon(x)$; (d) T_e.

From Tables 1–3 and Figs. 2–5, we can obtain the following points.

1) The homogenized solution gives the origin problem an asymptotic behavior, which is not enough for ε that is not so small. Hence, it is necessary to introduce the higher-order correctors. Table 3 and Figs. 2–5 show that the first-order and second-order correctors give a better approximation of the temperature and its gradient. The latter is even better than the former in approximation, especially at a high temperature or when the source term varies with large amplitude.

2) If the values of $k_{ij}^{\varepsilon}(x/\varepsilon)$ in different parts of the unit cells are all small, the homogenization results are not very good (see Cases 1–3). In these cases, we need to use the first-order, or even higher-order asymptotic approximations, especially at a high temperature. Furthermore, the proposed method is suitable for a very small periodic parameter ε. Namely, there are a great number of cells in a porous material.

3) From Tables 1 and 2, it is seen that the mesh partition numbers of the SOTS approximate solution are much less than that of refined FE solution, which means that the new approximate solution can greatly save computer memory and CPU time. Considering the advantage of the great reduction in computational efforts, the SOTS method is acceptable for the large scale simulations in practical engineering.

4. Conclusions

In this paper, a second-order two-scale computational method is developed for solving the conductive–radiative heat transfer problem in periodic porous materials. The SOTS formulation for the coupled problem is given, including the second-order two-scale asymptotic expression of the temperature field, and the formulations of the expected homogenized parameters.

Finally, the validity of the two-scale model is verified by comparing our method with the FE methods. By evaluating $N_{\alpha_1\alpha_2}(y)$, $C_{\alpha_1}(y)$, $C_{\alpha_1}^{1}(y)$, and $D(y)$, we can acquire more detailed information about the convection effects of pipes and radiation effects on the surfaces of the cavities and pipes walls, which indicates that the SOTS method can provide fairly accurate results with a great reduction of computational efforts. It could be useful for simulating the conductive–radiative heat transfer problem involved with a huge number of pores in practical engineering.

References

[1] Liu S T and Zhang Y C 2006 *Multidiscipline Modeling in Mat. and Str.* **2** 327
[2] Tiihonen T 1997 *Math. Method. Appl. Sci.* **20** 47
[3] Bakhvalov N S 1981 *Differ. Uraun.* **17** 1765
[4] Daryabeigi K 1999 37*th AIAA Aerospace Sciences Meeting and Exhibit*, January 11–14, 1999, Reno, NV
[5] Gibson L J and Ashby M F 1997 *Cellular Solids: Structure and Properties* (2nd Edn.) (Cambridge: Cambridge University Press)
[6] EI Ganaoui K 2006 *Homogénéisation de modèles de transferts thermiques et radiatifs: Application au coeur des réacteurs À caloporteur gaz* (PhD Thesis) (Ecole Polytechnique)
[7] Terada K, Kurumatani M, Ushida T and Kikuchi N 2010 *Comp. Mech.* **46** 269
[8] Mezedur M, Kaviany M and Moore W 2004 *AIChE J.* **48** 15
[9] Jen T C and Yan T Z 2005 *Int. J. Heat Mass Tran.* **48** 3995
[10] Xu R N and Jiang P X 2008 *Int. J. Heat Fluid FL.* **29** 1447
[11] Allaire G and EI Ganaoui K 2009 *Multiscale Model. Sim.* **7** 1148
[12] Allaire G and Habibi Z 2013 *SIAM J. Math. Anal.* **45** 1136
[13] Yang Z Q, Cui J Z, Nie Y F and Ma Q 2012 *CMES: Comp. Model. Eng.* **88** 419
[14] Bensoussan A, Lions J L and Papanicolaou G 1978 *Asymptotic Analysis for Periodic Structure* (Amsterdam: North-Holland)
[15] Oleinik O A, Shamaev A S and Yosifian G A 1992 *Mathematical Problems in Elasticity and Homogenization* (Amsterdam: North-Holland)
[16] Cui J Z and Yu X G 2006 *Acta Mech. Sin.* **22** 581
[17] Feng Y P, Cui J Z and Deng M X 2009 *Acta Phys. Sin.* **58** S327 (in Chinese)
[18] Han F, Cui J Z and Yu Y 2009 *Acta Phys. Sin.* **58** S1 (in Chinese)
[19] He W M, Qiao H and Chen W Q 2013 *Compos. Part B-Eng.* **45** 742
[20] He W M, Qiao H and Chen W Q 2013 *Eur J Mech ASolid* **40** 123
[21] Luo J L and Cao L Q 2004 *J. Engrg. Thermophys.* **29** 1711 (in Chinese)
[22] ShaoY F, Yang X, Zhao X and Wang S Q 2012 *Chin. Phys. B* **21** 083101
[23] Yu X X and Wang C Y 2013 *Chin. Phys. B* **21** 027101
[24] Amosov A A 2011 *J. Math. Sci.* **176** 361